
Copyright 2008, ABRACO

Trabalho apresentado durante o INTERCORR 2008, em Recife/PE, no mês de maio de 2008.

As informações e opiniões contidas neste trabalho são de exclusiva responsabilidade do(s) autor(es).

The Erosion-Oxidation Behavior of Commercial Steels AISI 1020, 410, 304 and 310 at High Temperatures

Stela M.C.Fernandes¹, Olandir V. Correa², Lalgudi V. Ramanathan³

Abstract

The high temperature erosion-oxidation (E-O) behavior of steels AISI 1020, 304, 310 and 410 was determined. These steels were selected to also evaluate the effect of chromium content on their E-O resistance. A test rig in which a specimen assembly was rotated through a fluidized bed of erodent particles was used to determine the E-O behavior. Alumina powder (200 μ m) was used as the erodent. The E-O tests were carried out in the range 25 - 600°C, with average particle impact velocities of 6, 14 and 30 ms⁻¹ at an impact angle of 90°. In the E-O tests, wastage of the steels varied with temperature and particle impact velocity (PIV). Depending on PIV, a transition in the dominant wastage mechanism occurred and the transition temperature varied with steel composition. Variation in Cr content of the steels did not affect wastage at low PIV. AISI 410 with 12% Cr revealed the lowest wastage at 30 ms⁻¹ compared to AISI 304 and 310. E-O maps of the steels were prepared as a function of PIV and temperature. Low, moderate and severe wastage zones were indicated in these maps to aid selection of these steels for industrial applications.

Key words: Erosion, erosion-oxidation, wastage, steels.

Introduction

The room temperature erosion behavior of metallic materials and ceramics has been widely studied. (1-3) The high temperature oxidation behavior of various metals and alloys is well documented but only limited information is available about the conjoint effect of erosion and oxidation at high temperatures. The results of some erosion-oxidation (E-O) studies have shown synergy between erosion and oxidation, indicating that degradation caused by E-O can be greater than the sum of degradation caused by erosion and oxidation operating separately.(4-6) There are also references to surface oxide scales inhibiting erosion.(7) That is, the wastage rate under E-O conditions are lower than that in the absence of oxidation. These contrary observations have generated, in recent years, increased attention about E-O processes. E-O interactions have been described in terms of regimes, often proposed as a function of temperature.(8-10) Definition of E-O regimes has varied significantly and so have the criteria for defining regime transitions.(11)

-
1. 1 Ph.D, Pesquisador, IPEN.
 2. Técnico, IPEN.
 3. Ph.D, Gerente do Centro de Ciência e Tecnologia de Materiais, IPEN.

Adequate procedures to select materials to resist E-O degradation at high temperatures are presently not available. Presently, a variety of metallic materials, composites, cermets and ceramics are used in industrial applications where E-O conditions prevail. The metallic materials include a variety of alloys meant for medium and high temperature applications. The criteria often used in many industries to select alloys for components subject to E-O conditions are hardness, cost and availability.

To provide further input to aid material selection for high temperature applications where E-O conditions prevail, studies were carried out to evaluate the E-O behavior of some commonly used steels with varying amounts of chromium. This paper presents the E-O behavior of AISI 1020, 304, 310 and 410. The E-O measurements were made in a test rig in the temperature range 25 - 600°C, using alumina particles as the erodent at average impact velocities of up to 30 ms⁻¹.

Methods and materials

Table 1. shows the chemical composition of the steels AISI 1020, 304, 310 and 410. Specimens 0.3 x 1.0 x 5.0 cm for the E-O tests were cut from the 'as-received' steel sheets, cleaned and degreased ultrasonically in acetone. A schematic diagram of the E-O test rig is shown in Figure 1. In this rig, a specimen assembly was rotated through a fluidized bed of erodent particles. Alumina powder with particles in the size range 212-150 µm was used as the erodent. The fluidized bed of particles was obtained by pumping pre-heated air through a porous plate supporting a bed of erodent particles. Fluidization of the erodent particles was done within a furnace and the erodent impact velocity on the test specimens was controlled by a motor that rotated the specimen assembly. The E-O test specimens were weighed and fixed with AISI 310 screws to the specimen holder in the E-O test rig. The specimens were positioned at the end of a crossed specimen holder. The E-O test conditions were: (a) temperatures - R.T., 100, 200, 300, 400, 500 and 600°C; (b) erodent particle impact angle of 90° at average velocities of 6 (V1), 14 (V2) and 30 (V3) ms⁻¹. After the tests, the specimens were weighed, examined in a scanning electron microscope and their surface reaction products analyzed by EDS.

Results and discussion

Erosion-oxidation behavior of the steels

Figures 2-4 show the wastage or weight loss of the steels as a function of E-O test temperature at the 3 particle impact velocities V1, V2 and V3.

Figure 2 shows that at particle impact velocity (PIV) V1, the wastage of the steels did not vary much up to 300° C. Above this temperature and up to 400° C all the steels except AISI 304 revealed an increase in wastage due to removal of both the surface oxide and the substrate by particle erosion. This increase in wastage was followed by a reduction in wastage at higher temperatures, indicating higher weight gain due to oxide formation than weight loss due to particle erosion. This transition took place at 400° C for AISI 310, at 450° C for AISI 1020, at 480° C for AISI 410 and at 510° C for AISI 304. At V2, shown in figure 3, the overall wastage was very low. All the steels revealed slight increases in weight up to 200° C and a behavior quite similar to that observed at V1. The Y-axis of this figure is expanded. Slight wastage could be observed in the temperature range 200-300° C, lower than that observed at V1.

This was attributed to two conjoint processes. Weight loss due to erosion and weight gain due to embedded particles on the specimen surface. In the temperature range 200-500° C, the slight variations in wastage of the steels were due to a combination of effects: oxide erosion, new oxide formation and embedded particles. Beyond this temperature range, a decrease in wastage was observed, and this marked the transition from the oxidation-aided-erosion-regime to the oxidation-controlled-regime.

Figure 4 shows the wastage behavior at V3. The wastage behavior is quite different, compared to that at lower PIV. Significant wastage was observed at temperatures up to 100° C, and due mainly to erosion of the surface oxide and the substrate. Above this temperature, the wastage decreased due to the combined effects of new oxide formation and embedded particles. The wastage of the steels AISI 1020 and AISI 410, both Fe₃O₄ and/or Fe₂O₃ formers, increased beyond 300° C, decreased after 400° C and again increased beyond 500° C. The other two steels, AISI 304 and AISI 310, both chromium dioxide formers, did not reveal this behavior. The wastage of these steels remained almost constant up to 500° C. All the steels revealed increased wastage above 500° C. This transition, observed at 500° C at V3 is the same as that observed at 300 or 400° C at V1. This increase in wastage, which takes place at higher temperatures with increase in impact velocity has been reported in other papers.(11) The shift to lower wastage observed at 400 C or 500° C at V1 probably occurs at V3 at temperatures above 600° C. The reduction in wastage at these temperatures is due to a transition from oxidation-aided-erosion-regime to oxidation-controlled-regime. Similar observations have been also reported. (11)

The oxide formed on the surface of AISI 1020 is a mixture of Fe₂O₃ and Fe₃O₄ at low temperatures and FeO at the higher temperatures. Fe₂O₃ is more ductile and with higher resilience to particle impact. On the other hand, FeO is brittle and easily removed upon particle impact. On the surfaces of the Cr containing steels, the oxide formed is a mixture of Fe and Cr oxides, depending on the Cr content of the steel. In the initial stages, the oxide formed is iron oxide and subsequently, the layers close to the metal-oxide interface consist of Cr₂O₃. The external iron oxide layer is easily removed by particle impact leaving behind a thin layer of Cr₂O₃. This process explains the reduced wastage at temperatures above 500° C. At even higher temperatures, the increase in wastage can be attributed to removal of the thin Cr₂O₃ layer along with the metallic substrate.

The troughs in the curves in figures 2 - 4 correspond to E-O regime transition. In the case of AISI 1020 it shifted from 450° C at V1 to 500° C at V2 to > 600° C at V3. In the case of AISI 410, the transition temperatures shifted from 500° C at V1 to > 600° C for V3. Inconsistencies in data related to V2 were observed and attributed to embedded particles. The transition temperatures for AISI 304 did not shift from 500° C with increase in particle impact velocity from V1 to V2. The transition temperature at V3 was > 600° C. In the case of AISI 310 the transition temperature shifted from 400° to 510° to >600° C with increase in PIV from V1 to V2 to V3.

Surface features of E-O tested steel specimens

The surfaces of all the steel specimens E-O tested at the various temperatures for 5 h and at the different PIV were examined in a SEM and specific regions were analyzed. The main surface were: (a) Embedded alumina particles on specimen surfaces (figure 5 a), and more so on specimens E-O tested at low temperatures. At higher temperatures few embedded particles were observed on the specimen surfaces. Similar observations were reported by Stack et. al. (12) (b) Erosion of the substrate (Figure 5 b); (c) The overall appearance of the E-O tested specimen surfaces were coherent with the wastage curves of the steels; (d) Platelet formation on the surfaces of all the steels E-O tested at 600° C and at V3. (Figure 6); (e) Effect of PIV on specimen surfaces was evident and the surfaces revealed substrate removal and platelet formation. (Figure 6)

The probable mechanism by which surface wastage occurred with increase in particle impact energy is illustrated schematically in figures 7 and 8.

Effect of Cr content on wastage of the steels

Figure 9 shows the wastage of the steels E-O tested for 5 h at 500° C as a function of chromium content in the steel. At V1, the wastage did not vary with Cr content of the steel. At V2, the wastage of all the steels increased, but the wastage decreased with the amount of Cr in the steel. The difference in the wastage of the steels AISI 410, 304 and 310 with 12, 18 and 25 % Cr is small. At V3, the wastage was significant. The presence of Cr in the steel decreased wastage markedly. However, AISI 410 with 12% Cr revealed the lowest wastage compared to AISI 304 and 310. This is due probably to formation of erosion resistant martensitic phases and chromium carbide precipitates in AISI 410.

Erosion-oxidation mechanisms

In general terms, wastage increases with increase in temperature up to a certain maximum value (critical temperature) and then decreases with further increase in temperature. This value in the wastage versus temperature curve shifts to higher temperatures and to higher wastage with increase in erosive particle impact energy and increase in oxidation resistance of the alloy. The reasons put forth to explain this behavior are many and one that has been widely accepted is : at low temperatures the dominant process is erosion of the metal and wastage is ‘erosion dominated’. With increase in temperature, oxide formation increases exponentially. That is

$$K_p = K_o \exp(-K/T)$$

Where K_p is the parabolic constant (assuming parabolic oxide growth), K_o and K are constants for a specific oxide and T the temperature.

If this oxide is significantly less resistant to erosion than the substrate, it is removed along with the substrate with increase in temperature at successive erosive events. since oxidation rates increase markedly with temperature this indicates that at a specific temperature the wastage due to loss of oxide is higher than wastage due to loss of metal.

This marks the wastage transition to ‘erosion-oxidation-dominated’. If the oxide continues to be removed by particle impact, the wastage increases with increase in temperature (increase in oxidation rate). However, at a certain critical temperature, the oxide formed between successive particle impacts attains a thickness and cohesion that are sufficient not to be removed to the oxide-metal interface. This marks the transition to ‘oxidation dominated’. Above this temperature the general loss of weight decreases with increase in temperature.

The results of this investigation indicate that the trough in the wastage curve, as a function of temperature shifts to higher wastage values and to higher temperatures with increase in particle impact velocities. The reason for this is that with increase in particle impact velocity, the time between impact events decrease and the energy of particle impact increases. The critical oxide thickness required for a transition in behavior from ‘erosion dominated’ to behavior that is ‘oxidation dominated’ should increase. Thus the temperature at which the critical oxide thickness is attained always happens at higher values with increase in temperature.

In certain cases, like AISI 410 and 304, in spite of the increase in wastage with increase in particle impact velocity, the depression in the corresponding wastage versus temperature curves did not shift to higher temperatures. This can be attributed to ‘tribologically caused

increase in oxidation' In the IPEN E-O test rig, the number of particles impacting the specimen surface increase with specimen rotation velocity. This possibility leads to a localized increase in oxidation of the surface due to localized heating caused by increase in particle flux. Consequently the critical oxide thickness is probably achieved at lower temperatures, compared with situations when there is no increase in oxidation due to tribological reasons. This effect has not been observed where particle flux is independent of its velocity. (8)

Erosion-oxidation maps

Wastage values in mg.mm² were specified to define low, moderate and high wastage. These values were based on data from literature about acceptable levels of degradation of industrial components exposed to aggressive atmospheres. Table 2 shows the wastage values to define the low, medium and severe wastage zones. On the basis of these values wastage maps were created as a function of temperature and erosive particle impact velocity in E-O conditions for the different steels. Figure 10 shows the E-O maps of the four steels. In these maps the low, moderate and severe wastage zones have been indicated with white, light grey and dark grey areas.

As a general orientation, the white and light grey regions in these maps indicate the temperature and particle impact velocity conditions under which these steels can be used for various applications in a number of industries. More data is required to improve these maps. These include: (a) lower and higher particle impact velocities; (b) other temperatures; (c) particle impact angles.

Conclusions

1. In the E-O tests at V1, the wastage of the steels varied significantly with temperature up to 300° C. Beyond this temperature and up to 400° C, all the steels except AISI 304 showed an increase in wastage due to loss of both surface oxide and the substrate by the impacting erosive particles. This increase in wastage was followed by a decrease at higher temperatures, indicating higher weight gain due to oxide formation than weight loss due to erosion. This transition took place at 400° C for AISI 310, at 450° C for AISI 1020, at 480° C for AISI 410 and at 510° C for AISI 304.
2. At V2, the overall wastage was low. All the steels showed a slight increase in weight up to 200° C. This was similar to that observed at V1. Low wastage was also observed in the range 200-300° C and was attributed to two conjoint processes, namely weight loss due to erosion and weight gain due to embedded particles. In the range 200 –500° C, the variations in wastage of the steels were due to a combination of effects: oxide erosion; new oxide formation and embedded particles. Beyond this temperature range, a reduction in wastage was observed marking the regime transition; from oxidation-aided-erosion-regime to oxidation-controlled-regime.
3. At V3, marked wastage was observed up to 100° C, due mainly to erosion of the air formed surface oxide and the substrate. Above this temperature, weight change due to oxide formation and embedded particles took place. The wastage of the Fe₃O₄/Fe₂O₃ formers, AISI 1020 and 410, increased at temperatures above 300° C, decreased beyond 400° C and once again increased above 500° C. Wastage of the chromium dioxide formers, AISI 304 and 310, remained almost constant up to 500° C. Above this temperature, all the steels revealed increases in wastage. This transition observed above 500° C at V3 was the same observed at 300° C or 400° C at V1.

4. The E-O transition temperatures of the steels as a function of PIV were determined. These temperatures for: (a) AISI 1020 shifted from 450° C at V1 to 500° C at V2 to > 600° C at V3; (b) AISI 410 shifted from 500° C at V1 to > 600° C at V3; (c) AISI 304 did not shift from 500° at V1 and V2 and shifted to > 600° C at V3; (d) AISI 310 shifted from 400° C to 510° C to > 600° C with increase in PIV from V1 to V2 to V3.
5. Variation in chromium content of the steels did not affect wastage at V1. The differences in wastage of the steels AISI 410, 304 and 310 with 12, 18 and 25 % Cr were small. At V3, the wastage of the steels with Cr decreased. However, AISI 410 with 12% Cr revealed the lowest wastage compared to AISI 304 and 310, due probably to the formation of martensitic phases and carbide precipitates in AISI 410.
6. Wastage values in mg.mm⁻² to define low, moderate and severe wastage were specified and based on these values E-O maps were prepared as a function of PIV and temperature. Low, moderate and severe wastage zones were indicated in these maps to aid in selection of these steels for industrial application.

References

1. SHEWMON, P.; SUNDERARAJAN, G. The erosion of metals, **Annual Review of Materials Science**, v. 13, p. 301, 1983.
2. BITTAR, J.G.A. A study of erosion phenomena, Part I. **Wear**, v. 6, p.5, 1963.
3. HUTCHINGS, I.M.; WINTER, R.E. Particle erosion of ductile metals – mechanism of material removal, **Wear**, v. 27, p.121, 1974.
4. WRIGHT, I.G.; NAGARAJAN, V.; HERCHENROEDER, R.B. Some factors affecting solid particle erosion/corrosion of metals and alloys, in Fall Meeting, Corrosion-Erosion Behavior of Materials', K. Natesan, ed., St. Louis, MO 1978. **Proceedings...**
5. LEVY, A.V.; ZAMBELLI, G. Particulate erosion of NiO scales, **Wear**, v. 68, p.305, 1981.
6. TABAKOFF, W. Experimental study on the effects of specimen sizes on erosion, **Wear**, v. 86, p.65, 1983.
7. STACK, M.M.; LEKATOS, S.; STOTT, F.H. Erosion-corrosion regimes: number, nomenclature and justification, **Tribology International**, v. 28, p.445, 1995.
8. KANG, C.T.; PETTIT, F.S.; BIRKS, N. Mechanisms in the simultaneous erosion-oxidation attack of nickel and cobalt at high temperatures, **Metallurgical Transactions**, v. 18A, p.1785, 1987.
9. RISHEL, D.M.; PETTIT, F.S.; BIRKS, N. Some principle mechanisms in the simultaneous erosion and corrosion attack of metals at high temperatures, **Materials Science and Engineering A**, v. 143, p.197, 1991.
10. STEPHENSON, D.J.; NICHOLLS, J.R. Modeling erosive wear, **Corrosion Science**, v. 35, p.1015, 1993.
11. STACK, M.M.; STOTT, F.H.; WOOD, G.C. Review of mechanisms of erosion-corrosion of alloys at elevated temperatures, **Wear**, v. 162-164(B), p.706, 1993.
12. STACK, M.M.; CHACON-NAVA, J.G.; STOTT, F.H. Synergism between effects of velocity, temperature and alloy corrosion resistance in laboratory simulated fluidized bed environments, **Materials Science and Engineering**, v.11, p1180, 1995.
13. WRIGHT, I.G.; NAGARAJAN, V.; STRINGER, J. Observations on the role of oxide scales in high-temperature erosion corrosion of alloys, **Oxidation of Metals**, 25, p175, 1986.

Table 1. Steel composition determined by x-ray fluorescence spectroscopy.

Steel	Elements (weight %)								
	C	Cr	Ni	Mo	Mn	Si	P	Cu	Fe
1020	0.15	-	-	-	0.33	-	-	-	Balance
304	0.07	18.7	8.0	0.03	1.4	0.6	0.04	0.09	Balance
310	0.07	24.1	19.1	0.07	1.7	0.5	-	0.1	Balance
410	0.04	11.5	0.18	-	0.14	0.5	0.4	-	Balance

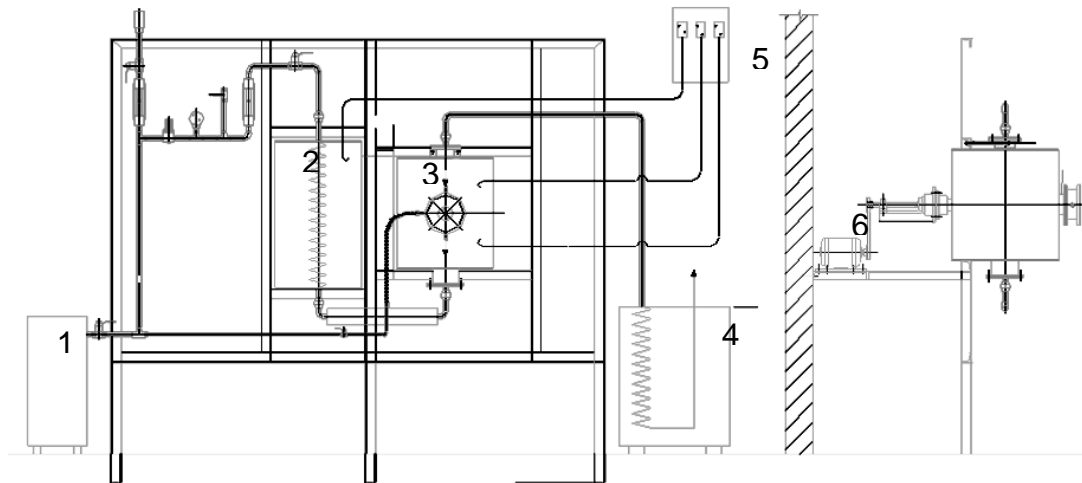


Figure 1. Schematic diagram of the erosion-oxidation test rig: 1- compressor; 2- pre-heating furnace; 3- E-O furnace; 4- system for retaining particles and for cooling; 5- control panel for controlling the motor and the furnaces; 6- motor to rotate the specimens through the bed of erodent particles in the furnace.

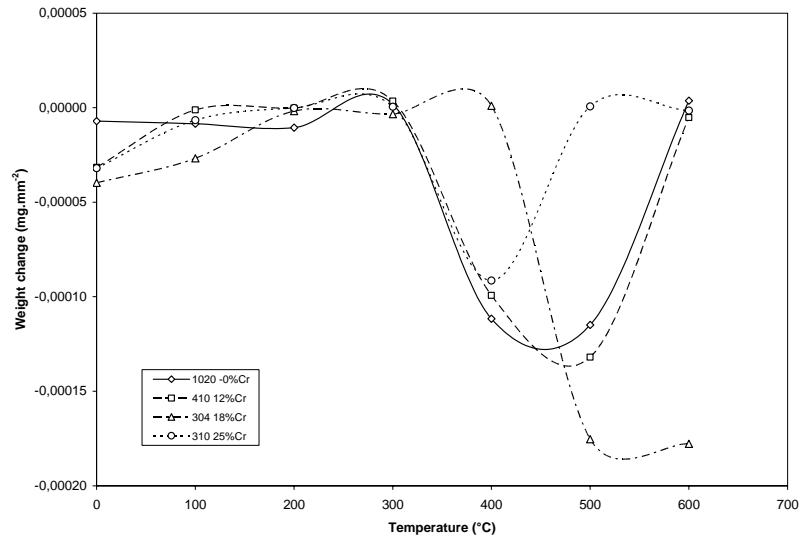


Figure 2. Wastage of the steels as a function of E-O test temperature with erosive particle impact velocity V1.

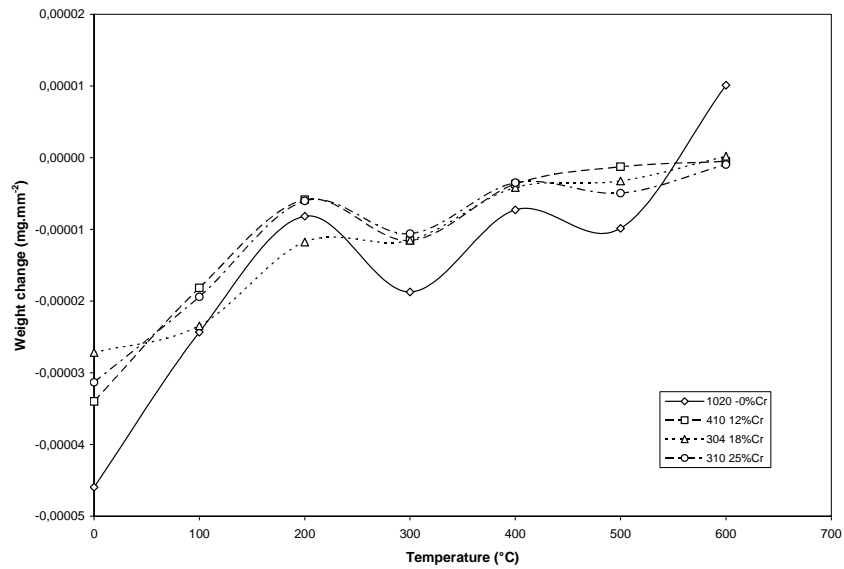


Figure 3. Wastage of the steels as a function of E-O test temperature with erosive particle impact velocity V2.

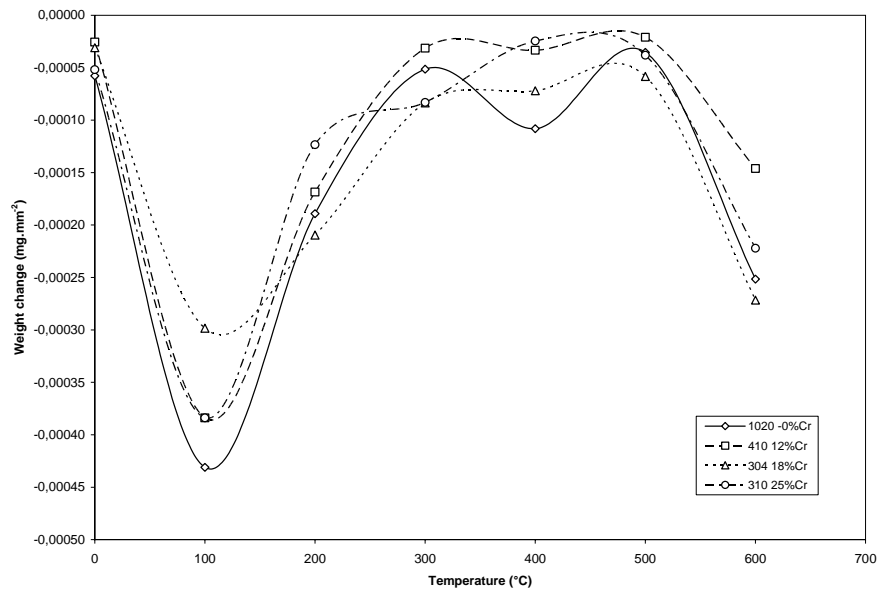


Figure 4. Wastage of the steels as a function of E-O test temperature with erosive particle impact velocity V3.

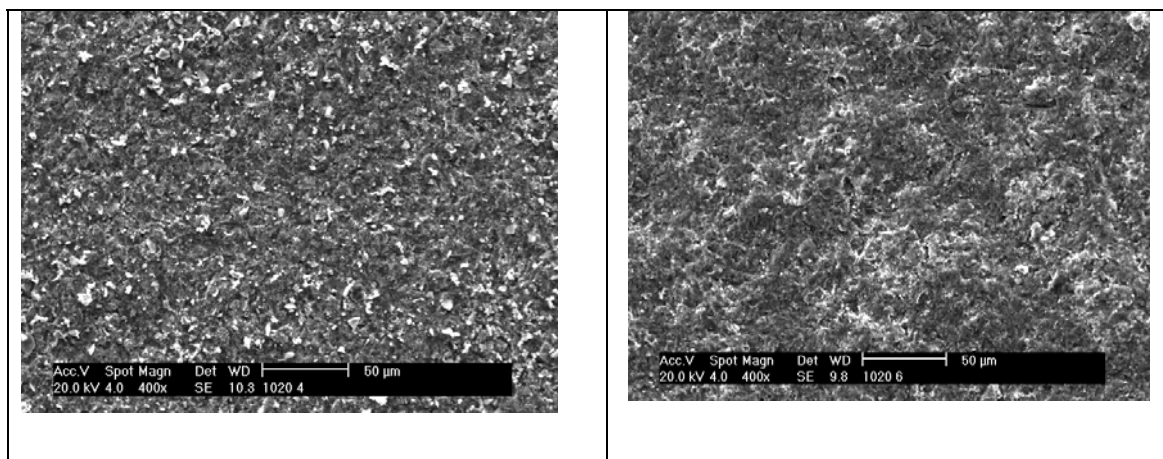


Figure 5. Scanning electron micrographs of AISI 1020 E-O tested for 5h at V1.
(a) 100° C, (b) 300° C.

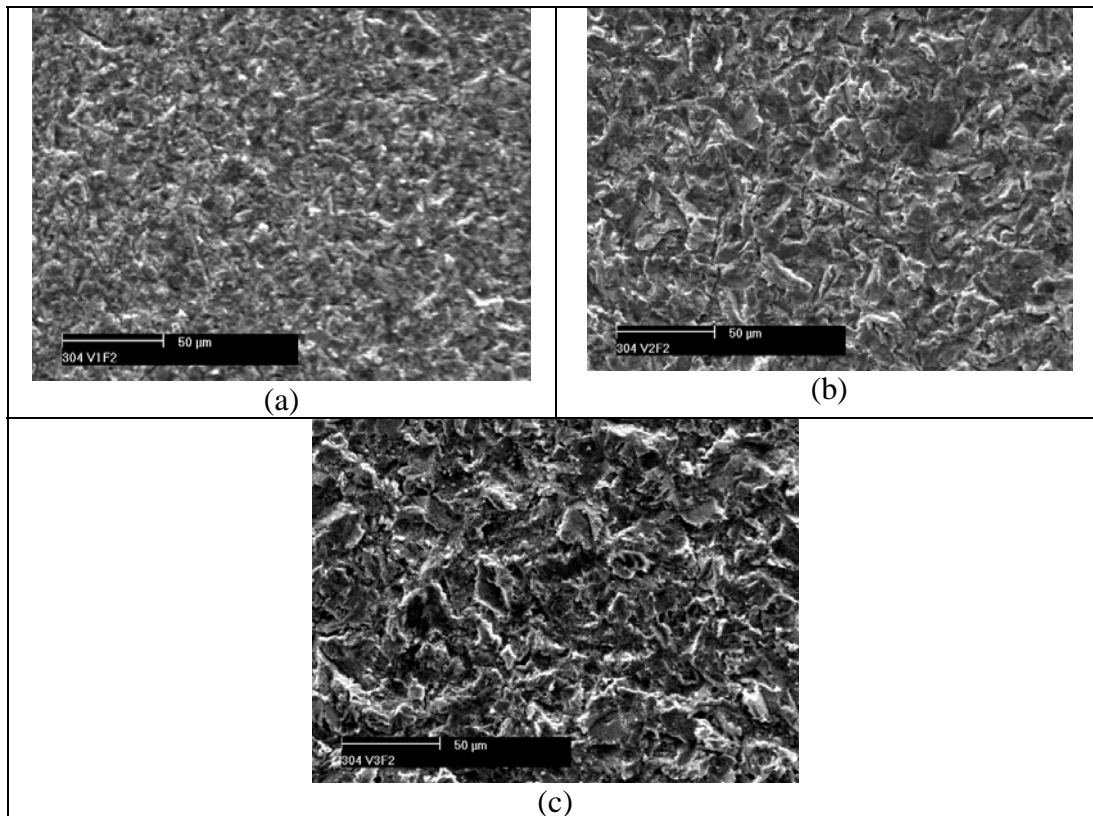


Figure 6. Scanning electron micrographs of AISI 304 E-O tested for 5 h at 500° C and at PIVs: (a) V1; (b) V2; (c) V3.

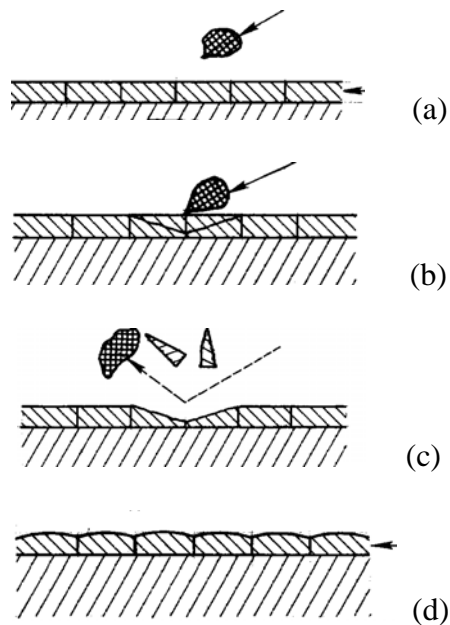


Figure 7. Schematic illustration of possible erosive events corresponding to low oxidation rates and low particle impact velocities resulting in oxide removal and accelerated oxidation.(13)

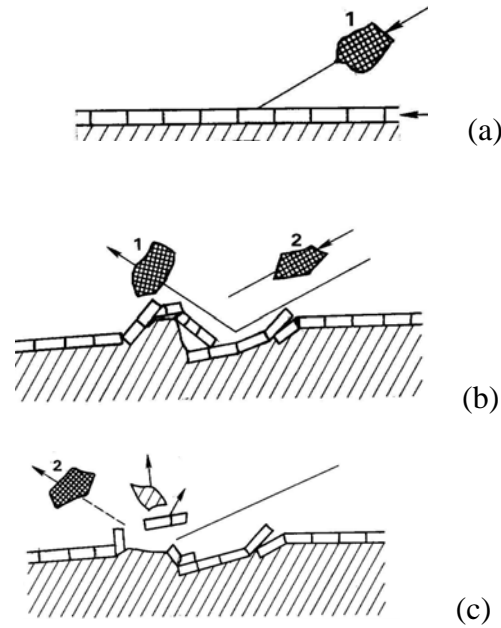


Figure 8. Schematic illustration of possible erosive events corresponding to low oxidation rates and high particle impact velocities resulting in formation of platelets and erosion-oxidation. (13)

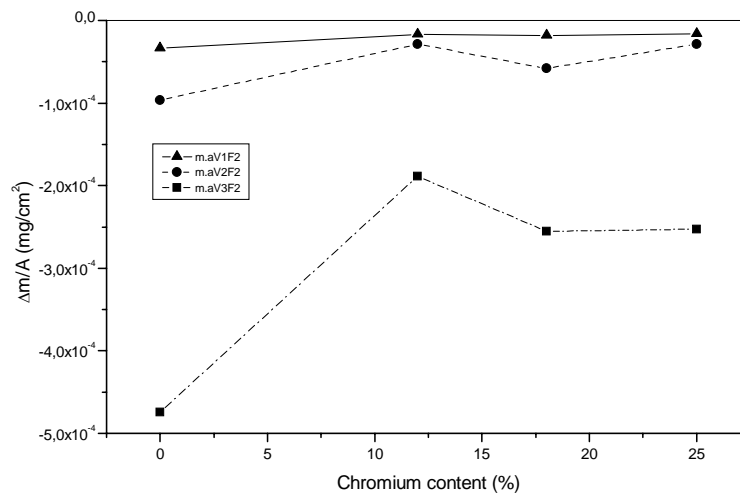
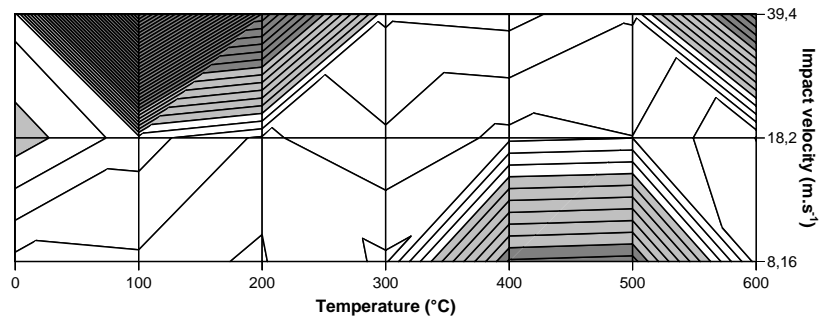


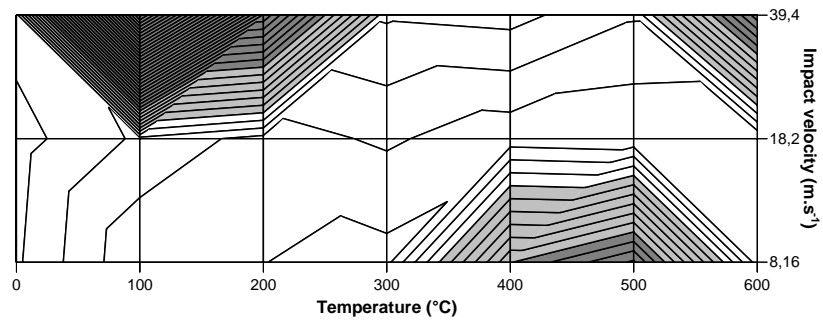
Figure 9. Wastage curves of the steels E-O tested at 500° C for 5h as a function of Cr content.

Table 2. Wastage levels to define low, moderate and severe wastage zones of the different steels.

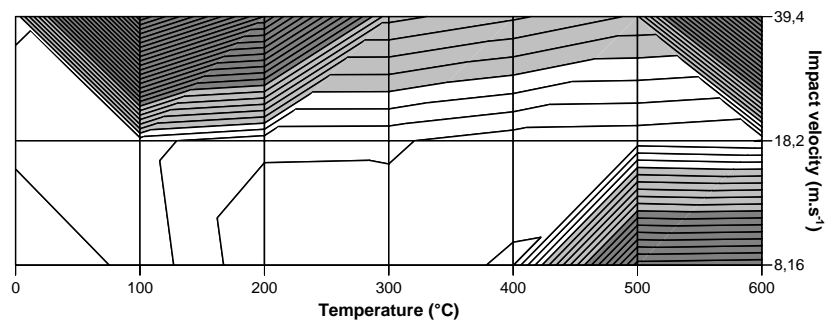
Wastage (mg.mm ⁻²)		
Low	Moderate	Severe
> - 4,0 x 10 ⁻⁵	> - 4,0 x 10 ⁻⁵ < -1,0 x 10 ⁻⁴	> -1,0 x 10 ⁻⁴



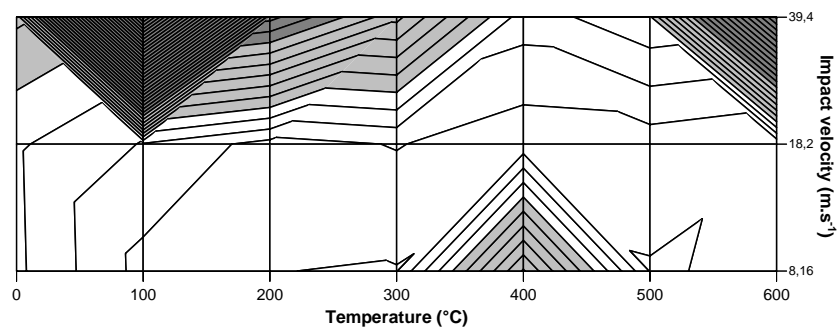
(a)



(b)



(c)



(d)

Figure 10. E-O wastage maps of the steels: (a) AISI 1020; (b) AISI 410; (c) AISI 304 ; (d) AISI 310.